Experimental Mechanics (2013) 53:299–317
DOI 10.1007/s11340-012-9633-1

The Potential for Assessing Residual Stress Using Thermoelastic Stress Analysis: A Study of Cold Expanded Holes

A.F. Robinson · J.M. Dulieu-Barton · S. Quinn · R.L. Burguete

Received: 12 December 2011 / Accepted: 23 May 2012 / Published online: 27 June 2012

Abstract Thermoelastic stress analysis (TSA) is a well established tool for non-destructive full-field experimental stress analysis. In TSA the change in the sum of the principal stresses is derived, usually when a component is subjected to a cyclic load. Therefore the mean stress or any residual stress in a component cannot be obtained from the thermoelastic response. However, modifications to the linear form of the thermoelastic equation that incorporate the mean stress may provide a means of establishing the residual stresses. It has also been shown that the application of plastic strain modifies the thermoelastic constant in some materials, causing a change in thermoelastic response, which may also be related to the residual stress. The changes in response due to plastic strain and mean stress are of the order of a few mK and are significantly less than those expected to be resolved in standard TSA. Recent developments in infra-red detector technology have enabled these small variations in the thermoelastic response to be identified, leading to renewed interest in the use of TSA for residual stress analysis in realistic components. The component studied in this work is an aluminium plate that contains a cold expanded hole, hence providing an opportunity to examine any changes in thermoelastic response caused by the residual stress in the neighbourhood of the hole. The variations in thermoelastic response due to residual stress are shown to be measurable and significant; validation of the residual stress field is provided by laboratory X-ray diffraction. The potential for a TSA based approach for residual stress analysis is revisited, and the feasibility of applying it to components containing realistic residual stress levels is assessed.

Keywords Thermoelastic stress analysis (TSA) · Residual stress · Cold expansion · Plastic deformation · Non-destructive.

A.F. Robinson · J.M. Dulieu-Barton (✉) · S. Quinn
Faculty of Engineering and the Environment,
University of Southampton,
Southampton SO17 1BJ, UK
e-mail: janice@soton.ac.uk

R.L. Burguete
Airbus Operations Ltd.,
New Filton House, Filton,
Bristol BS99 7AR, UK

Introduction

Residual stresses may be introduced into a component throughout the entire manufacturing process, so it is highly unlikely that an in-service component is entirely free of residual stresses. Since residual stresses are an almost unavoidable bi-product of manufacture, it is important to understand how residual stresses are distributed in a component; at present, there are several techniques available for measuring residual stresses. Destructive methods are not always practical for an in-service industrial environment, while non-destructive methods are typically expensive and time consuming. Therefore, demand for a cheaper and quicker non-destructive, non-contact, full-field residual stress evaluation technique is increasing, and thermoelastic stress analysis (TSA) [1] has been identified as a possible solution for a new, robust and portable means of non-destructive residual stress assessment.

Typical manufacturing residual stresses may be detrimental to a component's performance; however it is possible to enhance performance by introducing beneficial residual stresses. An example widely used in the aerospace industry is the cold expansion of holes to prevent fatigue crack growth and initiation by creating a region of compressive

residual stress around the hole edge. The residual stress distribution around cold expanded holes is relatively well defined, providing an opportunity to investigate variations in thermoelastic response due to residual stress, and assess the feasibility of applying a TSA based approach for residual stress assessment to realistic components.

TSA is a well established non-contacting analysis technique that provides full-field stress data over the surface of a cyclically loaded component. It is based on the small temperature changes that occur when a material is subject to a change in elastic strain, generally referred to as the 'thermoelastic effect'. When a material is subjected to a cyclic load, the induced strain produces a cyclic variation in temperature. An infra-red detector is used to measure the small temperature change, ΔT. Assuming ΔT occurs adiabatically, a relationship between ΔT and the change in the 'first stress invariant', $\Delta(\sigma_1 + \sigma_2)$, or the sum of the principal stresses [1] can be established as follows:

$$\Delta T = -KT_0\ \Delta(\sigma_1 + \sigma_2) \tag{1}$$

where T_0 is the absolute temperature and K is the thermoelastic constant, $K = \alpha/(\rho C_p)$, where α, ρ, C_p are the coefficient of thermal expansion, mass density and the specific heat at constant pressure of the material respectively.

As residual stress is essentially a mean stress, it is accepted that the linear form of the TSA relationship given in equation (1) does not allow its evaluation. However, there are situations where this linear relationship is not valid and these have enabled evaluations of residual stresses. Small variations in the thermoelastic response, resulting from the temperature dependence of the elastic properties, permitted the measurements. However, these changes in the thermoelastic response result in measured temperature change differences of a few mK, which are significantly less than those expected to be resolved in standard TSA. It was shown [2] that a revised form of the thermoelastic equation relating the rate of temperature change and the rate of change in stress can be written as:

$$\dot{T} = \frac{T_0}{\rho C_p}\left[-\left(\alpha + \left(\frac{\nu}{E^2}\frac{\partial E}{\partial T} - \frac{1}{E}\frac{\partial \nu}{\partial T}\right)\sigma_{kk}\right)\dot{\sigma}_{kk} + \left(\frac{(1+\nu)}{E^2}\frac{\partial E}{\partial T} - \frac{1}{E}\frac{\partial \nu}{\partial T}\right)\sigma_{ij}\dot{\sigma}_{ij}\right] \tag{2}$$

Where $\dot{T}$ is the rate of change of temperature, E is Young's modulus of the material, ν is Poisson's ratio and σ_{ij} is the stress tensor. Dotted terms in equation (2) represent a rate of change with respect to time. Essentially σ_{kk} is the mean stress, and $\dot{\sigma}_{kk}$ is the rate of change of the first stress invariant. The derivation of equation (2) also appears in [3] which is a review of the general theory associated with TSA. Equation (2) differs from equation (1) in that the elastic constants are not assumed to be temperature independent. It can be seen from equation (2) that the rate of change of the temperature is dependent on the rate of application of the stress, as well as the stress state, i.e. the mean stress. Hence, any dependence on the applied mean stress, as given by equation (2), is known to practitioners of TSA as the 'mean stress effect'; this terminology will therefore be used throughout the paper.

At present, three approaches have been investigated as potential candidates for residual stress measurement using the thermoelastic response [4]. Two of these are based on the relating mean stress in equation (2) to the temperature change or thermoelastic response. One utilises the thermoelastic response at the second harmonic of the loading frequency [5], and the other directly relates the change in the thermoelastic response to the principal stresses [6]. The mean stress effect was first observed by Belgen [7] and later confirmed by Machin et al. [8]. The revised higher order theory of the thermoelastic effect of equation (2) was proposed by Wong et al. [2], which accounted for the temperature dependence of elastic properties, and it was shown that the thermoelastic response is dependent on both the applied stress and the mean stress. The presence of residual stress within a component would form a contribution to the mean stress, and there would be a small difference in the thermoelastic response from that measured in the same component with zero residual stress, if subjected to the same loading conditions. While the mean stress effect is very small, it *has* been shown to be measurable in materials with temperature dependent elastic properties, including titanium (Ti-6Al-4 V), Inconel 718, and some grades of aluminium [9]. The major limitation of these two approaches is that they are not suitable for materials where the temperature dependence of the elastic properties around room temperature is negligible, e.g. some steels.

The third approach [10] is based on equation (1) and the change in the thermoelastic constant, K, resulting from plastic deformation during manufacture or assembly. Rosenholtz et al. [11], and Rosenfield et al. [12] have both demonstrated that in steel and aluminium, an application of plastic strain will cause a change in the coefficient of linear thermal expansion, α. Rosenfield et al. also noted that this change in α increases significantly when subjected to compressive strains, and increases less with tensile plastic straining. It has also been suggested that the change in α is affected by the strain hardening capability of the material [10, 13], i.e. the change in K for a material that *does* strain harden will be different than for a material that does not. In the third approach the main disadvantage is that plastic deformation must have taken place, but it has the advantage

that it may be valid for a larger range of materials, not just those with temperature dependent elastic properties.

A significant disadvantage common to all three approaches is that any change in the thermoelastic response resulting from either the mean stress or from the modification of K will be small. In actual components the changes in the response are around the noise threshold of the detectors. Previous success in detecting these changes has been achieved by applying very large residual stress or plastic strain, by using materials that are very sensitive to the mean stress effect, or from the investigation of specifically designed specimens. Recently there have been some major improvements in the functionality of infra-red detectors. The detector arrays are such that the fill-factor is practically 100 % providing a larger doped area increasing sensitivity, and in the case of the detector used in this work much faster sampling frequencies can be achieved as there are two detector readout circuits that output sequentially. This means that in general the temperature resolution has increased with less need to post-process the data, hence providing better spatial resolutions. Therefore it may now be possible to resolve the temperature changes representative of those in actual components, leading to a renewed interest in using TSA for residual stress analysis.

The present paper investigates the thermoelastic response around cold expanded holes in flat aluminium plates. TSA is conducted on a series of plates made from two types of aerospace grade aluminium alloy that contain a single circular hole. Each plate in the series contains a hole that has undergone a different amount of cold expansion, similar to those applied in the aircraft industry. Point by point comparisons of the thermoelastic response are made between plates that have experienced different amounts of cold expansion. Regions surrounding the hole that have a different thermoelastic response are identified using TSA, and then related to the areas affected by the cold expansion process. Validation of the residual stress field is provided by laboratory X-ray diffraction.

During cold expansion, the area around a hole experiences significant plastic deformation to introduce large compressive residual stress. It is possible that any variation in thermoelastic response between the cold expanded holes could be a result of a change in the effective mean stress, due to the presence of residual stress around the hole. In addition, since the area immediately adjacent to the hole has undergone significant plastic deformation, is it possible that this will effect α, and subsequently contribute to any change in thermoelastic response. To understand the origins of any changes in thermoelastic response, it is necessary to establish the mechanical and thermoelastic behaviour of both materials. The mean stress effect and the effect of plastic strain on the thermoelastic constant for each alloy is investigated using dogbone-type specimens loaded in uniaxial tension. Similarly, the effect of material directionality (due to cold rolling) and strain hardening (due to alloy composition) on the thermoelastic response is also examined. In addition, since the variations in thermoelastic response are very small, it is important to minimise sources of signal attenuation and understand the possible sources of error within the measurement; a discussion of these sources is presented and optimum conditions for the TSA are suggested.

Cold Expansion Process

The cold expansion process [14] is an established means of generating a beneficial compressive residual stress distribution around a hole to prevent fatigue crack growth and initiation. It has also been shown to inhibit the growth of existing cracks. The cold expansion process entails plastically deforming the material directly adjacent to the hole to develop compressive residual stress [14]. The split-sleeve expansion method is most commonly used, and involves pulling an oversized tapered mandrel through an internally lubricated split-sleeve that has been positioned inside the hole, as shown in Fig. 1 [15]. The combined thickness of the sleeve and mandrel relative to the size of the hole controls the amount of expansion. The hole undergoes forced expansion to cause plastic deformation, and as the mandrel is removed the material undergoes partial, but not full recovery, due to the permanent deformation that has occurred. The material further from the hole which is only elastically deformed, springs back from the expanded state and forces

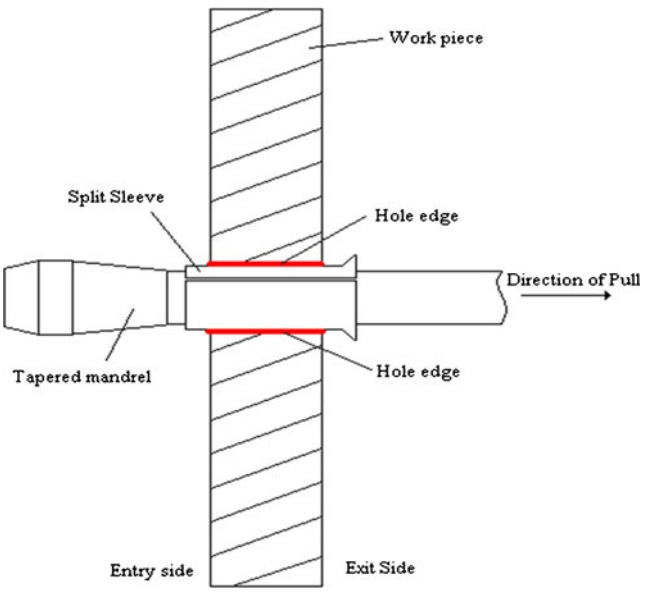

Fig. 1 Schematic of the split sleeve cold expansion method

the plastically deformed material closer to the hole into compression. Consequently, a large beneficial compressive residual stress is formed close to the hole, which reduces with distance away from the hole edge, as shown in Fig. 2 [16]. During the process, as the mandrel is removed, the material on the entry side of the hole begins to relax, however the material on the exit face does not, since it is still constrained by the presence of the mandrel. As a result, the final residual stress distribution is three-dimensional with a different magnitude of residual stress on the entry and exit sides of the hole [17]. There are many features that influence the residual stress field around a cold expanded hole, and although the shape is well defined, it can be difficult to quantify the final distribution. Some of the influencing factors include: method of expansion, level of expansion, specimen material, plate thickness, and the location of the hole relative to edges and other holes.

A plate containing a cold expanded hole has been chosen for this investigation for a number of reasons. It is a realistic engineering component that is widely used and relevant to industry, which provides a complex stress field that is three dimensional in nature. Furthermore, plane stress solutions exist for the applied loading conditions (which can be corrected for finite dimensions), and the residual stress distribution around a cold expanded hole is relatively well defined. This enables previous work to be explored within the context of a more realistic stress field, and for results to be validated against existing knowledge and solutions.

In the study described in the present paper, the test specimens are aluminium plates containing a single central hole that has been cold expanded using the split-sleeve method,

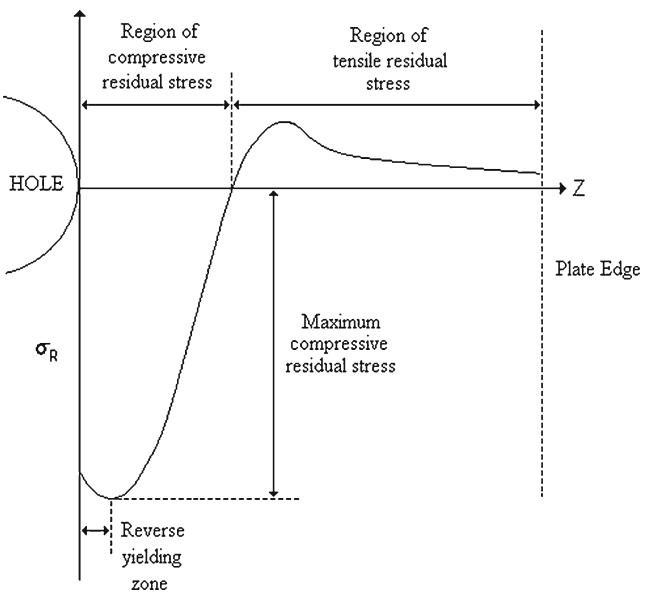

Fig. 2 Typical tangential residual stress profile around a cold expanded hole

described above. The optimum level of cold expansion using this method is 4 % [18]. The holes were cold expanded by 2 % and 4 %, and then reamed to a final diameter; a plate containing a reamed hole that had not been expanded was used as a reference specimen, i.e. 0 % expansion. Provided the plates experience the same loading conditions in a controlled environment, any variation in the thermoelastic response from around the holes must be due to the presence of residual stress caused by the cold expansion process. From previous studies that use TSA to investigate residual stresses, the variations in the thermoelastic response have been identified as being caused by either: (a) the mean stress effect, (b) the effects of plastic strain on the thermoelastic constant, or (c) a combination of both. In order to assess the feasibility of a TSA based approach to residual stress assessment it is important to establish the contribution of these effects and ascertain which, if either is dominant.

Experimental Methodology

The primary objective of this work is to observe variations in thermoelastic response around cold expanded holes due to the presence of residual stress, attribute these changes to either the mean stress effect, plastic deformation, or both, and ultimately to assess the feasibility of using TSA as a means of detecting residual stresses within actual components. To supplement the investigation of cold expanded holes, it is necessary to perform a series of dynamic and static tensile tests to characterise the mechanical and thermoelastic behaviour of the materials under investigation; this involves loading dog-bone type specimens in uniaxial tension to achieve the following:

a) Obtain mechanical properties and ascertain the temperature dependence of the elastic properties for each alloy (at room temperature).
b) Assess the effect of the mean stress on the thermoelastic response in each alloy.
c) Determine the effect of plastic deformation on the thermoelastic constant, K, for each alloy and establish the significance of strain hardening.
d) Examine any material directionality that is present due to cold rolling and investigate what affect this has on the thermoelastic response.

In a dog-bone type specimen loaded in uniaxial tension, the stress can be calculated in a straightforward manner as force divided by cross-sectional area. It is then possible to obtain the thermoelastic constant, K, from equation (1) as the applied stress is known and ΔT and T values can be obtained from the infra-red detector. In particular, this methodology has been used for determining the effect of plastic

strain on the thermoelastic constant for the following three reasons:

(i) If this type of specimen is loaded beyond the material's yield point and then unloaded, it will result in a residual strain; however, there will be no residual stress as the stress can be fully relaxed by the elastic unloading. Without a residual stress that would result in an increase in the mean stress when loaded, any change in the thermoelastic response would be due to a change in one of the material properties, α, ρ or C_p, and not due to the mean stress effect. It should be noted that at the change in cross-section near the clamped ends there will exist a strain mismatch, and therefore a residual stress will be developed upon unloading; however, this will likely be small, highly localised, and well away from the area under inspection.

(ii) For a specimen loaded in cyclic uniaxial tension, non-adiabatic conditions cannot occur because there is no stress gradient, and therefore there is no heat transfer within the specimen.

(iii) Since the stress in a specimen loaded uniaxially can be calculated, the change in thermoelastic constant due to plastic deformation can be obtained. For a specimen containing a known amount of plastic strain a thermoelastic constant, K_P, can be derived. K_P can then be compared to K for a specimen containing no plastic deformation, K_0.

The parameters used to manufacture the plate specimens, which contain the cold expanded holes, have been chosen to be representative of in-service applications. The geometry of the plate, e.g. thickness, hole diameter etc., are as used in the manufacture of aircraft, whilst the cold expansion process is also typical. However, considerations such as the limitations associated with the load capacity of the available test machines, and the necessity to impart a uniform load through loading jigs are also considered. The specimen dimensions are given in Table 1 and the specimen geometry and the loading jig are shown in Fig. 3.

The aluminium plate specimens were manufactured with dimensions of 300 mm by 150 mm by 10 mm and contained a hole of nominal diameter 5/8″ (15.875 mm). These dimensions were chosen for two reasons: firstly, the distance from the edge of the plate relative to the diameter of the hole (*e/D* ratio) is sufficiently large (i.e. greater than 3) for edge effects to not cause any unusual variation of the residual stress distribution during the cold expansion process [16]. Secondly, it was shown in [19] that infinite plate conditions (i.e. no edge effects during cyclic loading) could be achieved if the distance from the hole to the plate edges (*d1* and *d2*) is greater than 3.3*D* and 6.7*D* in the x and y directions respectively. Although this does not consider the finite thickness of the plate, which causes a reduction in the surface stresses.

To assess the influence of the amount of strain hardening a material experiences on the thermoelastic response, two grades of aluminium are investigated. One material that is reported to experience a large amount of strain hardening is AA2024-T351 and one which does not strain harden significantly is AA7085-T7651, hence these materials were chosen.

In total, 8 plates were manufactured from each aluminium alloy; 4 containing a cold expanded hole, and 4 additional plates from which the dog-bone type tensile specimens were manufactured. Holes were cold expanded to 2 % and 4 % and reamed to a final diameter; one plate containing a 4 % cold expanded hole was left unreamed, and one hole was reamed but not cold expanded to provide a reference specimen, i.e. 0 %. It should also be noted that the mandrel split was aligned with the top of the hole, and that prior to cold expansion, the plates had been cold-rolled (in the 300 mm direction). Tensile specimens had a nominal cross sectional area of 15 mm by 5 mm and were cut at 0°, 45° and 90° to the rolling direction.

For the TSA, an Instron 8802 servo-hydraulic test machine with a load capacity of 100 kN was used to cyclically load each specimen; a Cedip 480 M infra-red detector was used to obtain thermoelastic data. For the static loading procedures, an Instron 5569 servo-mechanical test machine with a load capacity of 50 kN was used (unless specified otherwise); strain gauges were bonded to measure strain within the gauge length of the specimens where necessary.

Investigation of Experimental Conditions for TSA

The magnitude of the change in thermoelastic response associated with residual stress is very small, so it is

Table 1 Specimen dimensions

Plate specimens			Dog-bone specimens		
A	Plate length	300 mm	L_1	Gauge length	70 mm
B	Plate width	150 mm	W_1	Gauge width	15 mm
C	Attachment holes	6 mm	L_2	Specimen length	150 mm
D	Hole diameter	15.875 mm (5/8″)	W_2	Specimen width	25 mm
d1	Edge distance (x)	4.7 *D*	L_3	Tab length	35 mm
d2	Edge distance (y)	9.4 *D*	*R*	Radius	5 mm
h_1	Plate thickness	10 mm	h_2	Specimen Thickness	5 mm

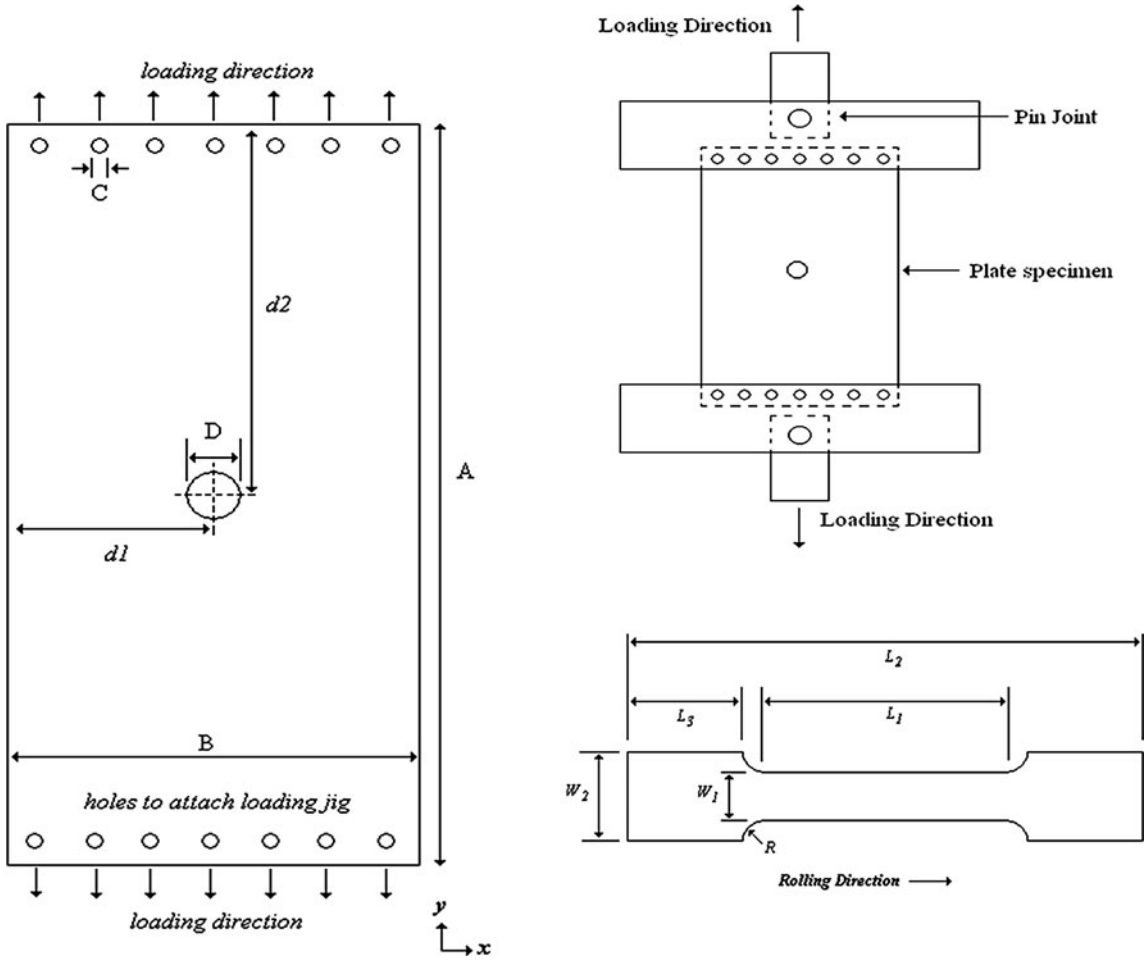

Fig. 3 Plate specimen dimensions and loading mechanism

necessary to examine potential sources of error. It is known that the major factors influencing the change in thermoelastic response (and subsequently K) are the high emissivity coating, background temperature, applied stress and the infra-red detector settings; these effects must always be considered in parallel to any evaluations of the significance of changes in response due to mean stress or from the modification of K. Therefore a study of these factors was conducted using dogbone-type specimens loaded in uniaxial tension (for the reasons described in the previous section), to provide an understanding of the potential errors and noise sources in the measured data.

High Emissivity Coating

Metallic specimens are typically coated with a thin layer of matt black paint to provide a suitable surface for TSA, and it is known that the coating could cause attenuation of the thermoelastic response if not prepared correctly. There are three main reasons for using a high emissivity coating [20]. Firstly, to achieve a consistent emissivity on the surface; any variation of surface emissivity across the specimen would cause a variation in the temperature change that is not stress related. The second reason to use a high emissivity coating is to maximise the radiant energy being emitted; since the temperature changes are very small, a high emissivity will yield a stronger and more accurate signal. Thirdly, a high emissivity coating is used to avoid reflected heat radiation; if the surface is too reflective, radiation from external sources may appear as emission from the specimen surface. McKelvie [21] discussed two important types of paint coating attenuation, thermal lag and thermal drag-down; it was shown that as paint thickness and loading frequency increase, there is a decrease in the thermoelastic signal due to these coating effects. Significant work investigating the effects of the surface coating on a range of metallic materials has been completed and is documented in [22]. The effects of coating characteristics have been investigated for AA2024, and quantitative guidance for paint thickness and loading frequency have been defined. In this work, a thin layer of RS matt black paint was applied to the surface of all specimens in accordance with preparation guidelines

established in [22]. The paint thickness ranged between approximately 16 μm and 21 μm and was measured using a CMI153 paint coating thickness gauge.

Infra-red Detector Settings

To obtain T and ΔT from the detector output, it is necessary to apply a radiometric calibration routine. This is done using experimentally derived and certificated curves supplied by the manufacturer in the form of a look-up table in the system software. The detector is calibrated annually using a series of black bodies of known temperature, therefore the error in T and ΔT is considered negligible when compared to the system noise. The noise equivalent temperature difference (NETD) of the Cedip Silver 480 M system is 18 mK; however, for TSA a lock-in technique is used that enables further processing, allowing the NETD to be reduced to approximately 4 mK [23]. By employing long data collection and integration times, and careful monitoring of the experimental conditions this can be reduced further. To fully assess the sources of noise within the detector setup, the following detector parameters were investigated: non-uniformity correction, data capture frame rate, integration time, number of images recorded, camera temperature, background temperature and the influence of background effects. Table 2 shows the variation of ΔT due to a change in each detector property. It should be noted that whilst each parameter is investigated independently, some are intrinsically linked, for example, a change in frame rate or integration time requires a new non-uniformity correction to be performed. All data was collected from the same specimen under the same loading conditions, and the specimen was not removed between tests.

Table 2 indicates that background effects and background temperature have the most significant influence on the measured temperature data. Variation of the other detector properties yielded typical changes in ΔT of the order of 1 to 2 mK. During all TSA, large black cloths were positioned around the specimen to shield it from any background radiation, providing a uniform background emissivity. Assessing the influence of background effects was achieved by recording data with and without the shielding present. It should be noted that experiments examining the influence of all other parameters, and all work associated with establishing variations in thermoelastic response around cold expanded holes, were conducted *with* the shielding present, thus the effect of background effects can be considered negligible in these investigations. If the variation of background or camera temperature is large (i.e. 5 °C), a difference in the measured ΔT values of several mK could be seen. Typically, recording thermoelastic data takes a matter of seconds, and therefore the changes in background temperature are very small; a change in T of approximately 10 to 20 mK could be expected. The difference in background temperature over a series of tests may be as much as 1 K, which is unlikely to cause significant variation of the response. However, the variation of background temperature between data recorded on different days in an uncontrolled environment may be significant. It is clear that if very high accuracy is required, comparisons should not be made between data sets recorded under different experimental conditions; this includes different detector settings, and different environmental conditions. It is therefore very important to monitor the background temperature to ensure large variations are not occurring.

Any changes that may be caused by variation of detector properties are not relevant to the main work since all tests were completed under the same test conditions; additionally, during the test period changes in background and camera temperature were minimal, and thus its influence is considered negligible. The detector settings used for the remainder of this work were as follows: 1050 recorded images, with an integration time of 1300 microseconds, at a frame rate of 383 Hz.

Table 2 Typical variation of thermoelastic response due to a change in detector properties

Parameter	Variables	Variation of ΔT [mK]	% variation
Integration Time [μs]	800, 1300, 1800	2–8	0.6–3
Frame rate [Hz]	131, 257, 383	1–3	0.3–0.8
Number of images	400, 800, 1050	0–1	0–0.3
Non-uniformity correction (NUC)	#1, #2, #3	0–2	0–0.6
Background effects	With/without shielding	8–24	3–8
Background/Camera temperature [°C]	21–25	4–8	1–3

Applied Stress

Another possible error source is the calculation of the applied stress from prescribed loading conditions. The cross-sectional area of each tensile specimen was obtained using callipers accurate to 20 μm and by measuring at a number of positions and taking the average; the subsequent error is negligible. The test machine is calibrated annually by the manufacturer using standard procedures, and the error in the load output is very small. In addition, an angle-meter was used to ensure correct vertical alignment of the specimens, and therefore it is concluded that any error in the calculation of the applied stress can be considered negligible in this work.

Material Characterisation

Acquiring a complete knowledge of the material behaviour, both mechanically and thermoelastically is an important step

in understanding the mechanisms causing the variations in thermoelastic response around the cold expanded holes. The present section outlines the work undertaken to characterise both grades of aluminium alloy and establish the magnitude of the effects discussed previously in the experimental methodology section.

Mechanical and Thermoelastic Properties

Obtaining the yield strength, ultimate tensile stress and % strain hardening was achieved by quasi-statically applying load until failure at a rate of 0.5 mm min^{-1}. The modulus of elasticity was measured using the same method, while ensuring the load did not exceed the elastic limit of the material. A strain gauge (EA-13-120LZ-120) was mounted on both sides of the specimen and the test repeated six times. To obtain the baseline thermoelastic constant, tensile specimens of each aluminium alloy were cyclically loaded at a mean load of 8 kN (107 MPa), with a load amplitude of 4 kN (54 MPa). Tests were conducted at 5 Hz, 7.5 Hz and 10 Hz to assess the effect of the paint coating on the recorded data.

Table 3 shows the relevant mechanical and thermoelastic properties of the two aluminium alloys obtained from tensile specimens. Five specimens of each alloy were used to obtain the data, and the values shown are the average over all five specimens; numbers in brackets represent the largest variation seen within each set of tests. AA2024 strain hardened by 32 % and AA7085 by approximately 9 %, confirming the different strain hardening characteristics of the two alloys (where the ability to strain harden is defined by the percentage increase of the ultimate tensile strength in comparison to the yield strength).

Mean Stress Effect

It has been shown [13] that the mean stress effect is largely governed by the temperature dependence of the elastic modulus ($\partial E/\partial T$), and thus for a material whose elastic properties are not very temperature dependent, the mean stress effect will be very small. It has been reported [24] that a mean stress effect has been measured in some grades of aluminium. It is therefore necessary to establish the temperature dependence of E, and investigate the extent of the mean stress effect in both alloys specific to this investigation.

A thermal chamber was fitted to the test machine to facilitate testing within a temperature controlled environment, and specimens aligned at 0° to the rolling direction were quasi-statically loaded to approximately 10 kN (133 MPa) and then unloaded. A strain gauge (CEA-13-125UT-350) was mounted on both sides of the specimen to monitor the strain throughout each test. The modulus of elasticity was calculated from the gradient of the elastic region of the stress–strain curve at temperatures ranging from 20 °C to 60 °C in increments of 10 °C. Six repeat tests were conducted at each temperature and the results shown in Fig. 4. Tests were then conducted just above room temperature to populate the curve further at 5 °C intervals in regions where it may be practical to conduct TSA measurements.

A reduction in elastic modulus with increasing temperature was measured in both grades of aluminium, and while the value of $\partial E/\partial T$ at room temperature for each alloy suggests that the mean stress effect will not be large, it may still be of significance in this work. Tensile specimens were cyclically loaded at 10 Hz, with a load amplitude of ±3 kN (40 MPa) about a series of different mean loads; these ranged from 4 kN (54 MPa) to 19 kN (253 MPa) for the AA2024 alloy, and from 4 kN to 31 kN (413 MPa) for the AA7085 alloy, in increments of 3 kN. The maximum permitted mean load was governed by the yield strength of the material since the material must not exceed its elastic limit. The effect of the mean stress is shown in Fig. 5, and the increase in thermoelastic response due to the mean stress is clearly evident. For an increase in mean stress from 54 MPa to 253 MPa for AA2024, the increase in ΔT was approximately 10 mK, and for an increase in mean stress from 54 MPa to 413 MPa for AA7085, the increase in ΔT was approximately 20 mK. Since there was a small increase in background temperature from the initial to final test, the calibrated thermoelastic response, ΔT, has been divided by the background temperature, T, in Fig. 5. $\Delta T/T$ was calculated using equation (2) and literature values for α, ρ and C_p, measured values of $\partial E/\partial T$ were used and $\partial v/\partial T$ was assumed zero in accordance with the experimental findings. It can be seen that the theory values and those derived in the experiment are similar, hence verifying these results for the two aluminium alloys.

The effect of the mean stress has been shown to be of measurable magnitude in both grades of aluminium. The residual stress around the cold expanded holes would be expected to be of a similar order to the mean stress, and thus could cause differences in the measured thermoelastic response between the holes that have and have not been cold

Table 3 Mechanical and thermoelastic properties of AA2024-T351 and AA7085-T7651

Material	Yield stress [MPa]	Ultimate tensile stress [MPa]	% Strain hardening	Modulus of elasticity [GPa]	Thermoelastic constant, K [Pa^{-1}]
AA2024-T351	352 (±5)	464 (±3)	31.8 (±1.8)	74.8 (±0.2)	9.8×10^{-12} (±0.05)
AA7085-T7651	494 (±6)	538 (±9)	8.9 (±1.2)	69.2 (±0.4)	9.4×10^{-12} (±0.06)

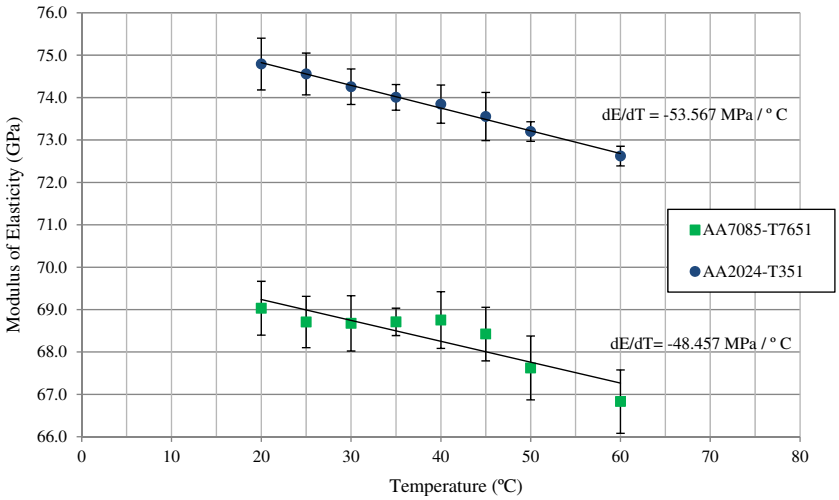

Fig. 4 Temperature dependence of elastic modulus (*dE/dT*) for AA2024 and AA7085

expanded by modification of the effective mean stress. Therefore the effect of mean stress warrants consideration in this study.

Effect of Plastic Deformation on *K*

It has been shown that plastic strain causes a change in the coefficient of thermal expansion, α, and therefore will modify *K*. If the change in *K* can be defined over a range of plastic strain, it may then be possible to establish the plastic strain that has been experienced based on a measured change in *K* from a reference value. The materials ability to strain harden, and any directionality may also affect the change in *K,* and therefore specimens of both alloys, aligned at 0°, 45°, and 90° to the rolling direction were investigated.

To obtain the change in *K,* a set amount of plastic strain was applied to each tensile specimen, followed by cyclic loading to obtain the thermoelastic response, and thus K_P was calculated. The desired levels of plastic strain (2 % and 4 %) were achieved by loading and unloading at a rate of 0.5 mm min^{-1}. A strain gauge (EA-13-120LZ-120) was mounted on one side of the specimen and an Imetrum video-extensometer was used on the opposite side to measure the strain during the plastic deformation procedure. A calibration specimen was used to obtain the thermoelastic constant, K_0, for 0 % strain for each material. A Cedip Silver 480 M infra-red detector system was used to measure *T* and ΔT from each specimen. A cyclic load with mean load of 8 kN (107 MPa) and a load amplitude of 4 kN (54 MPa) at 10 Hz was applied to the specimens.

Figures 6 and 7 show the variation of K_P/K_0 for AA2024 and AA7085 specimens aligned at 0°, 45° and 90° to the rolling direction. It can be seen that the change in K_P/K_0 is different for each alignment direction, and that the effect of plastic strain is greatest for the 45° specimen; the smallest change was measured for the 0° direction. The error bars were calculated by combining the standard deviation of the ΔT and *T* values within the area of interest enabling a

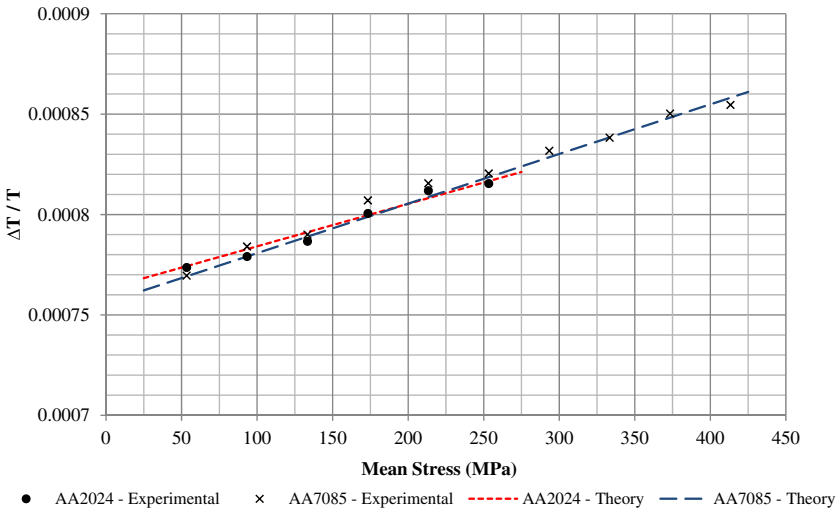

Fig. 5 Mean stress effect in AA2024 and AA7085

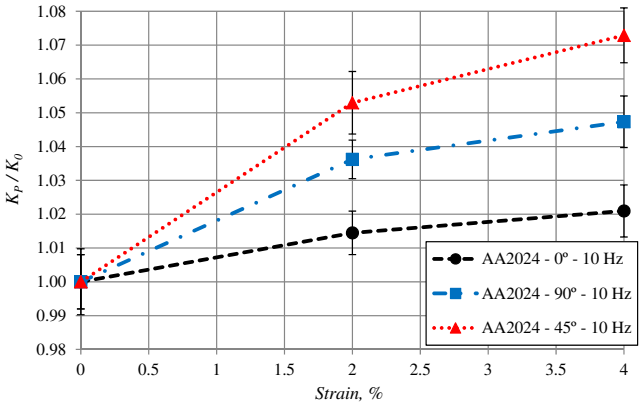

Fig. 6 Variation of K_P/K_0 for different specimen orientations for AA2024

calculation of the maximum and minimum values of K_P, which were then normalised by the corresponding value of K_0. While the temperature changes associated with this effect are very small (approximately 5–15 mK for the data shown), it can be seen that K_P/K_0 increases with increasing levels of plastic strain for each material. For specimens aligned with the 0° direction the change in K_P/K_0 is larger in AA7085 which does not strain harden significantly; conversely, for the 90° and 45° specimens the change in K_P/K_0 is larger for the AA2024 material, which *does* exhibit more strain hardening. In the previous work [10] the relationship between strain hardening and the change in K_P/K_0 was proposed to explain the differences between the materials inspected, however the material directionality was not considered. Conversely, in the current study which has explored directionality, it is noted that there is no clear effect of strain hardening on the change in K_P/K_0 due to plastic deformation. Since it is assumed that the density and specific heat remain constant, it can be inferred that the change in thermoelastic constant due to plastic strain is a result of a change in α. It was speculated that small differences in the microstructure

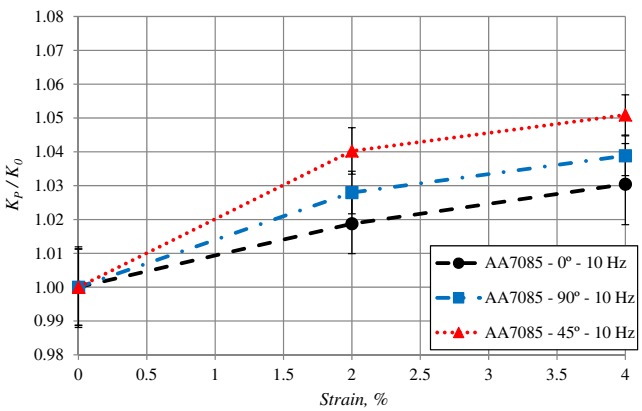

Fig. 7 Variation of K_P/K_0 for different specimen orientations for AA7085

between the strained and unstrained specimens may provide an insight into the physical processes causing the change in K_P/K_0 and how material directionality influences this change.

The largest change in K_P/K_0 was measured between the AA2024 specimens aligned at 45° to the rolling direction, and the smallest change was noted in the AA2024 specimens aligned at 0°. These specimens were identified as the most likely to reveal any noteworthy differences, and therefore the most appropriate for microstructural investigation. A central section measuring approximately 15 mm by 15 mm of the strained (4 %) and unstrained (0 %) AA2024 specimens aligned at 0° and 45° was removed and mounted in Bakelite resin. This section corresponded to the location of the strain gauge used during the deformation procedure. The samples were polished, followed by etching in Keller's solution (95 ml water (H_2O), 2.5 ml nitric acid (HNO_3), 1.5 ml hydrochloric acid (HCl), 1 ml hydrofluoric acid (HF)) for approximately 10 s. The microstructure of each specimen is shown in Fig. 8(a) to (d). It can be seen that there is significant elongation of the grains in the 0° direction in both the strained and unstrained specimens; this material had been cold rolled and stress relieved by stretching during its fabrication. It is not possible to identify any modification of the grain structure from a comparison of the micrographs, and thus difficult to link the application of strain and the change in K_P/K_0 to any change in microstructure. In the specimens cut at 45°, the same elongation of grains in the 0° direction is shown; comparison of the strained and unstrained specimens did not reveal any elongation or reorientation of grains in the direction of loading. The microstructural investigation indicates that grain reorientation due to the loading may not be responsible for the change in thermoelastic constant with respect to rolling direction.

Due to the differences in K_P/K_0 for different alignment directions, it is apparent that knowledge of material directionality would be required to enable an evaluation of plastic strain based on a change in thermoelastic constant from a reference specimen. The plates containing cold expanded holes have been cold rolled and the direction is known, however the stress distribution is more complex than for a tensile specimen, such that a calibration based on K_P must account for the anisotropic characteristics of the mechanical behaviour of the material. Nevertheless, the fact that plastic deformation has occurred is likely to change the measured thermoelastic response. Moreover, in cold expansion the relaxation is constrained, and thus residual stress is also present; this is in contrast to tensile specimens where there is no residual stress since it could be relaxed during unloading. Furthermore, the area around the cold expanded hole will have experienced compressive plastic strain, and therefore a similar but negative change in K_P is expected. Unfortunately, it was not possible to obtain K_P/K_0 for compressive plastic strain due to limitations with specimen design and

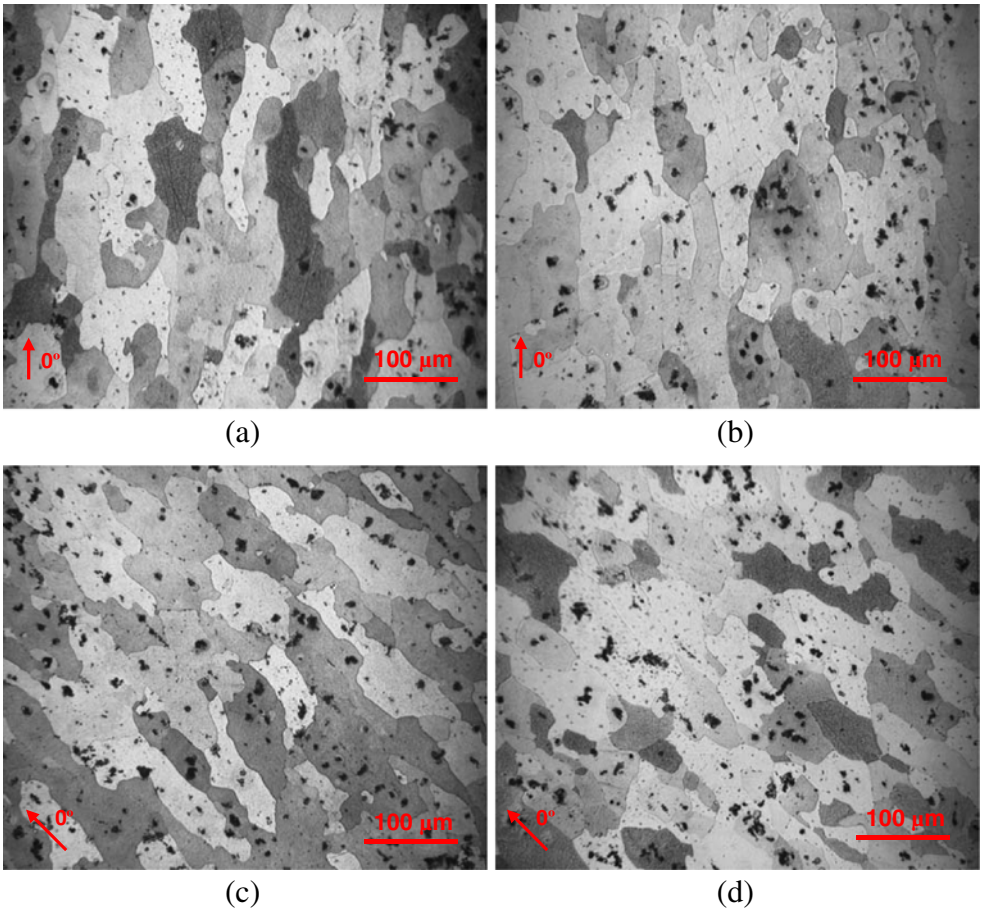

Fig. 8 Microstructure of AA2024-T351 specimens with different amounts of plastic strain. **a** Specimen aligned at 0° with 0 % strain, **b** Specimen aligned at 0° with 4 % strain, **c** Specimen aligned at 45° with 0 % strain, and **d** Specimen aligned at 45° with 4 % strain

the available material. However, the change in K_P/K_0 for compressive strain can be estimated, and is based on previous work [12] where the change in α was seen to be negative and slightly larger for compressive strain in comparison to the equivalent tensile strain and confirmed by current work examining stainless steel 316 L, where an increase in K_P/K_0 was seen for tensile plastic strain, and a larger decrease for compressive plastic strain.

TSA around Cold Expanded Holes

Plate specimens were cyclically loaded (in the rolling direction) at a mean load of 30 kN, with a load amplitude of 25 kN and a frequency of 10 Hz. Thermoelastic data was recorded from both the entry and exit faces of the plate, at two viewing distances: (i) at a stand-off distance of 385 mm, showing the hole as well as areas of uniform stress away from the hole, and (ii) at a stand-off distance of 200 mm, showing only the area immediately adjacent to the hole.

The 2 % and 4 % cold expanded holes would be expected to contain large compressive residual stress very close to the hole (within a few mm) reducing to small tensile residual stress further from the hole, as shown in Fig. 2. Away from the hole, the residual stress state would be similar to that in the 0 % plate, as they have all be cut from the same cold rolled piece of material. Any differences in thermoelastic response due to residual stress should be identifiable from comparison of the thermoelastic data. It was ensured that the infra-red detector was positioned such that the location of the hole remained the same in each test, thus allowing a pixel by pixel comparison of the thermoelastic data for each plate. Due to the large dynamic load range, some rigid body motion was noticeable in the TSA video data and this was particularly apparent at the specimen edges. A motion compensation routine based on image analysis was performed which removed the errors associated with the motion. The motion compensation was achieved using the Random Motion software provided by the infra-red system manufacturer; the procedure operates by identifying two significant and contrasting features in the first frame of the recorded data, which are then tracked through subsequent frames allowing them to be rotated, distorted or translated such that any motion appears stationary.

Figure 9 shows TSA data observed from around 0 %, 2 % and 4 % cold expanded holes on the entry sides of AA7085 plates; the stress sum distribution that would normally be expected around a hole is clearly identifiable. The circular

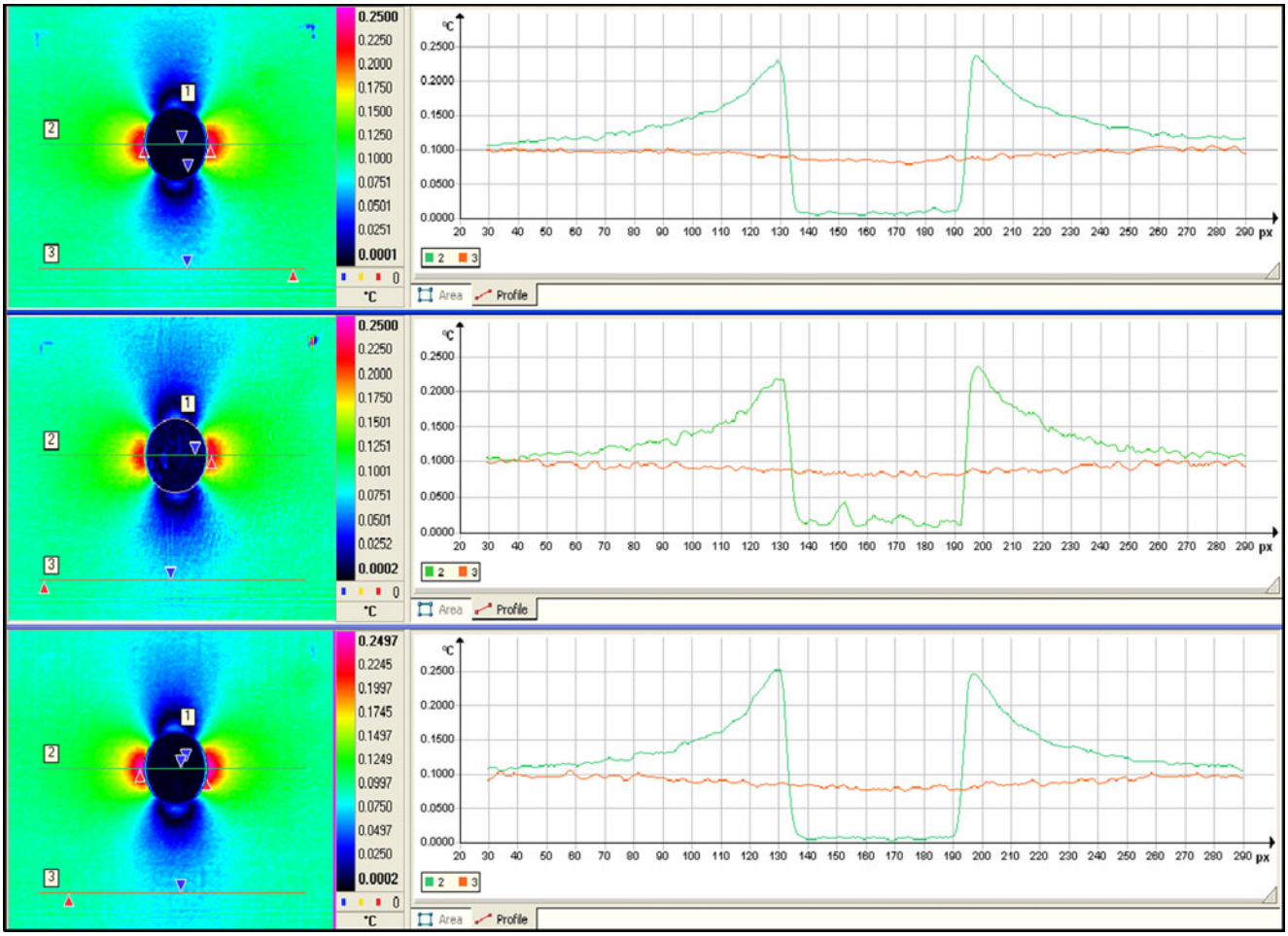

Fig. 9 Thermoelastic response around cold expanded holes in AA7085-T7651 plates, Entry side loaded at 10 Hz; (*Top*) 4 %, (*Middle*) 2 %, (*Bottom*) 0 %

area {1} was applied to each image to check the hole was in the same position and that motion compensation was successful. During each test, the hole was filled with plasticine, which shows little or no thermoelastic response and thereby provides a well-defined edge to allow a clear identification of the hole in the data. Two line plots have been taken from the data; the first {2} shows the thermoelastic response directly across the hole, the second {3} shows the response further from the hole, in a region of more uniform stress. For the reference specimen (0 %), it can be seen that the background temperature change is approximately 0.10 °C and the maximum temperature occurring at the hole edge is approximately 0.25 °C. Using equation (1) and the thermoelastic constant for AA7085 in Table 3, the applied stresses can be approximated as 35 MPa in the plate and 90 MPa at the hole. (A stress concentration factor of 3 cannot be expected from a non-infinite plate and the influence of finite conditions are detailed later in the paper.) In an ideal situation, increasing the applied load would increase the stress, and thus increase the differences in the temperature changes that are of interest. However, further increasing the applied load could result in some areas containing tensile residual stress exceeding the elastic limit, as well as approaching the load capacity of the test machine, and other deleterious effects arising from bending or distortion of the loading rig at high cyclic loads.

To examine differences in thermoelastic response, ΔT data around the 0 % cold expanded holes was subtracted from the data around the corresponding 4 % cold expanded holes on a pixel by pixel basis; this formed new data sets ($\Delta T_{4\%} - \Delta T_{0\%}$) revealing areas with a different thermoelastic response (Fig. 10). Note, the data from within the holes has been removed, along with the immediate edge data that may be spurious due to edge effects. From Fig. 10(a), clear differences in the thermoelastic response from around the 4 % and 0 % cold expanded holes can be seen in the new data sets. The markings seen in the top left and top right corners of each image correspond to paint that was scratched from the surface to provide reference points for motion compensation.

An evaluation of the background noise caused by the subtraction process is required; a line of data from an area of uniform stress in each 0 % plate was subtracted from the same area on the corresponding 4 % plate. This provides an

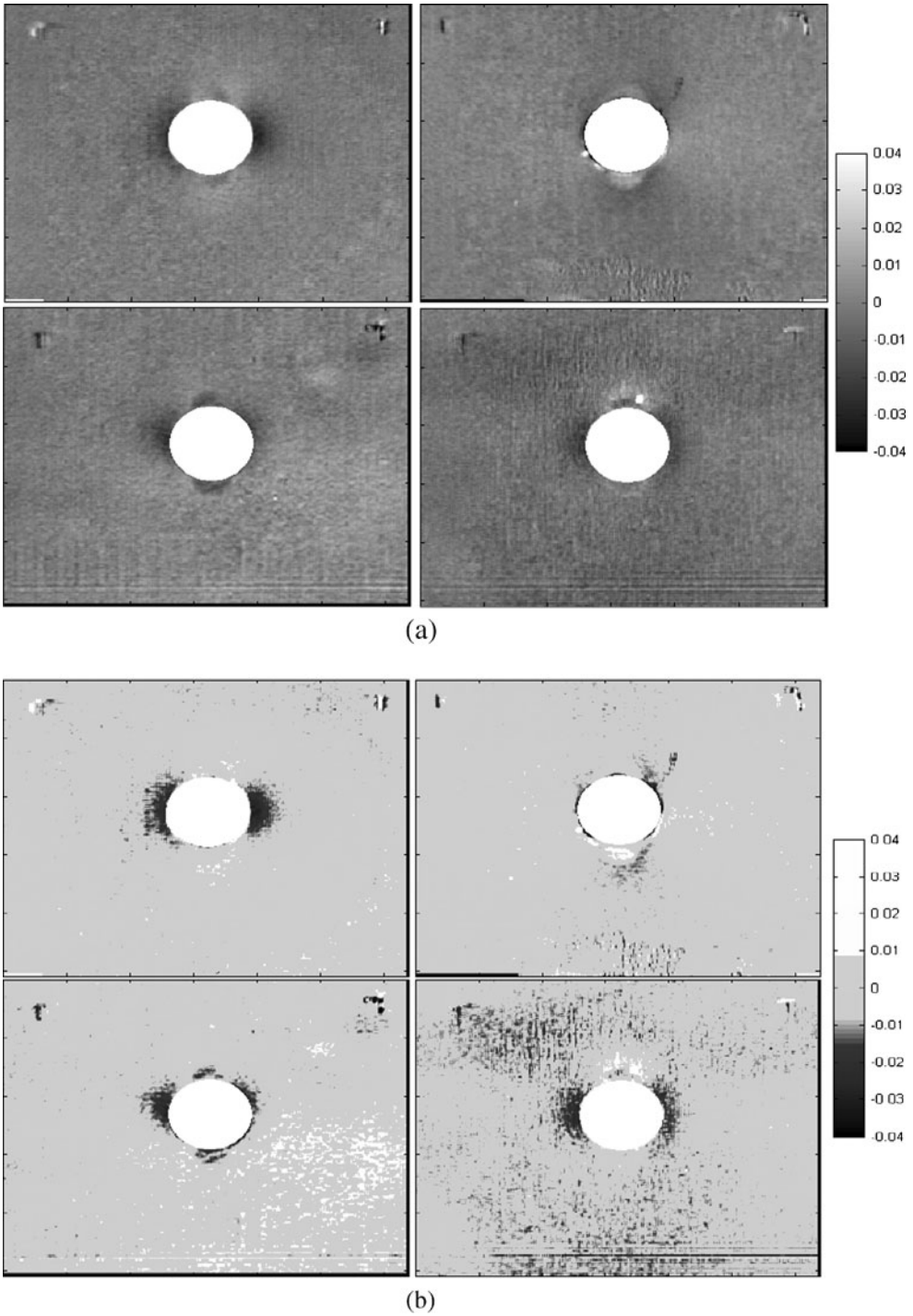

Fig. 10 Difference in thermoelastic response around the 4 % and 0 % cold expanded holes, ($\Delta T_4 - \Delta T_0$). **a** Without threshold noise filter applied, **b** With threshold noise filter applied. (*Top left*) AA2024 entry, (*Bottom left*) AA7085 entry, (*Top right*) AA2024 exit, (*Bottom right*) AA7085 exit

estimate of the difference in background thermoelastic response, which in turn provides an estimate of the noise content in the subtracted data set. Any variation of the thermoelastic response falling within the maximum and minimum values (typically ±0.006 K) was disregarded as potential noise from subtraction. By applying these limits to each new data set, it is possible to obtain an image where departures in the thermoelastic response between identically loaded plates of the same material can be identified. Even though the subtraction noise is relatively large in comparison to the changes in thermoelastic response that are of interest and it is possible that some effects may be masked by this process, for large plastic strain and large residual stress the variation would be expected to be of greater magnitude (10 to 20 mK). Figure 10(b) shows the $\Delta T_{4\%} - \Delta T_{0\%}$ data sets for the entry and exit sides of the AA2024 and AA7085 plates with the threshold noise filter applied. The variations in ΔT are small, but it is encouraging that

measurable differences exist that are larger than the estimated noise content, and far enough from the hole edge not to be a result of erroneous measurement or edge effects. The changes are also similar in magnitude to those measured due to the mean stress effect and plastic deformation in tensile specimens of the same material.

Since the loading conditions are the same for each plate, the difference in the thermoelastic response between the specimens must be a result of the residual stress around the hole caused by the cold expansion process. The expected residual stress profile (Fig. 2) would take the form of a ring of compressive residual stress close to the hole, with a very small region of different residual stress directly above the hole corresponding to the location of the split in the sleeve. The data for the AA7085 entry side and the AA2024 exit side show variations in ΔT around the hole correlating well with the expected areas of residual stress. However a different distribution is seen for the AA7085 exit side and the AA2024 entry side which is similar to the applied stress. It may also be considered that as the distribution follows what would be expected from the applied stress field, what is being observed in the data may be a consequence of the mean stress.

Validation of Residual Stress using Laboratory X-ray Diffraction and Comparison with the Theoretical Thermoelastic Response

The cold expansion process yields a relatively well defined residual stress distribution in the vicinity of a hole and it has been shown that small changes in the thermoelastic response can be identified in the regions where residual stress is expected. However, the extent of the residual stress in the neighbourhood of the holes is unknown. Therefore laboratory X-ray diffraction (XRD) has been used to quantify the residual stress field around the cold expanded holes. The purpose of this validation is three-fold. Firstly, to verify that cold expansion has taken place and to compare the residual stress profile across the hole to that expected from Fig. 2. Secondly, to investigate the uniformity of the residual stress distribution around the hole and compare with the TSA results in Fig. 10. Finally, by obtaining quantitative values of residual stress, it will enable it to be accounted for in a theoretical evaluation of the thermoelastic response and hence permit a validation of the experimental results.

Residual stress measurements were taken at various locations around the 4 % cold expanded holes in both aluminium alloys, and on both the exit and entry faces of each plate. Measurement points included a horizontal line through the centre of the hole, at distances of 1 mm, 3 mm, 6 mm, 10 mm and 15 mm from the hole edge, enabling comparison of the distribution with that in Fig. 2. Further measurements were taken radially around the hole at intervals of 30° at a distance of 3 mm from the hole edge to observe the uniformity of the residual stress profile and assess the success of the cold expansion procedure. The residual stress was also measured local to the split in the split sleeve, where a slightly different level of residual stress would be expected. The plate was orientated such that the rolling direction was aligned with the y-axis, and the location of the split was located at the bottom of the hole (i.e. a negative y-direction). The residual stress measurements were obtained using a Proto L-XRD machine and a chromium K-alpha radiation source with a wavelength of 2.29 Å. The elastic constants were, $1/2S_2 = 19.54 \times 10^{-6}$ Pa^{-1} and $S_1 = -5.11 \times 10^{-6}$ Pa^{-1}, the reflection plane {311} and the nominal Bragg angle was 139°. The density of aluminium was taken as 2,780 kg m^{-3} and the useful penetration depth of the measurements is estimated to be approximately 25 μm. Data was obtained for two orientations at each point, Phi=0° and Phi=90° (i.e. in the x and y directions).

The tangential residual stress profile for the entry and exit sides of the AA2024 and AA7085 plates containing 4 % cold expanded holes is shown in Figs. 11 and 12 respectively. It can be seen that there is good symmetry in terms of the residual stress profile either side of the hole, and also that the distribution in similar to that which would be expected from Fig. 2. In addition, a difference in magnitude between the entry and exit faces can also be seen, and are designated by E and X respectively. The level of residual stress around the circumference of the hole was consistent, with a slight increase in the region coinciding with the location of the split in the sleeve. From the distribution of residual stress shown in Figs. 11 to 12 it can be concluded that the cold expansion process was successful, confirming that large amounts of compressive residual stress is present immediately adjacent to the hole, which reduces with distance away from the hole edge. It can also be concluded that the differences in shape and magnitude between the data sets shown in Fig. 10 are not caused by inaccuracies from cold expansion.

Unusually, the maximum residual stress is consistently larger on the entry side of the plates for both materials. This is contrary to expectations where it would be typical for the largest residual stress to be present on the exit side. The unexpected result has no effect on the outcome of the work in the paper and therefore has not been further explored in the present work. It may be that the prior effect of cold rolling has changed the resultant residual stress after cold expansion, or quite simply that the plates were incorrectly marked during the manufacturing process. However, it should be noted that the actual orientation of the plates is largely irrelevant for this work. The same notations have been used from the outset for both the TSA and X-ray diffraction procedures and therefore it is known which diffraction measurements relate to which TSA measurements. The purpose was to quantify the residual stress that was

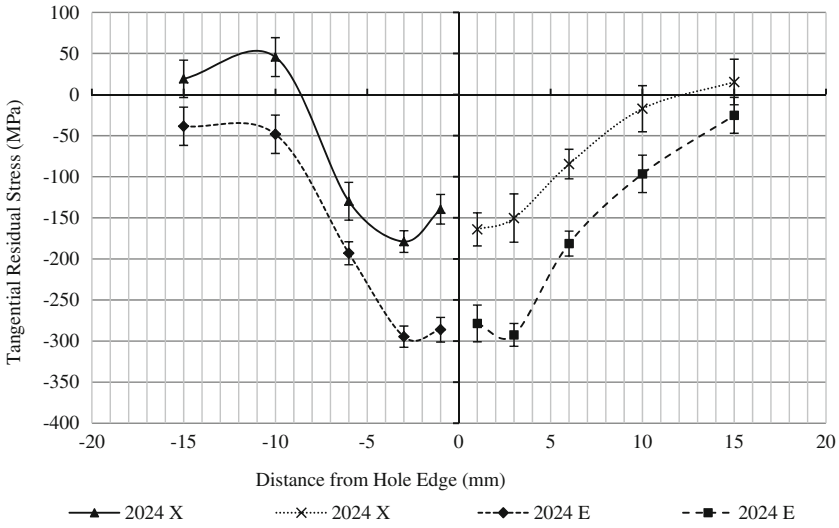

Fig. 11 Tangential residual stress along horizontal line through centre of hole for AA2024

present on each side of the plate for input into the fundamental equations and facilitate a comparison with TSA data; this has been achieved and comparison of theoretical and experimental data is now possible.

With knowledge of the residual stress distribution and the material properties obtained previously, it is possible to use equation (2) to obtain the theoretical thermoelastic temperature change for a line across the hole. In addition, by modifying the mean stress terms in equation (2), the theoretical change in temperature for the case with residual stress (i.e. with 4 % cold expansion) and the case without residual stress (0 %) can be obtained. This can then be compared with the experimental temperature changes obtained from TSA.

The stress distribution around a hole in a flat plate loaded uniaxially is readily obtained from literature [25]. However, an analytical solution exists only for an infinite plate, and therefore a correction must be made to account for the finite dimensions of the plate used in this work. Using data from [26-28] a correction has been applied that reduces the stress concentration factor at the hole from 3 for an infinite plate subject to plane stress, to 2.72 for the finite dimension plates used in this work. This accounts for the hole diameter to plate width ratio, and the thickness to hole diameter ratio. It should be noted that the plate is too thick relative to the hole diameter to allow plane stress conditions to be assumed, but too thin to allow plane strain assumptions, and thus the modification that accounts for the finite dimensions of the plate is not perfect. Figure 13 shows a comparison of the theoretical and experimental stress distribution along a horizontal line extending 30 mm from the hole edge in the plate with a hole that has not been cold expanded. The theory has been calculated using the known applied stress, and results for both the corrected and original analytical solution are shown; the experimental data obtained using TSA are also shown. The experimental data correlates well with the modified theoretical distribution and is therefore considered acceptable to use for the comparison of further experimental data collected from the plates with the cold expanded holes.

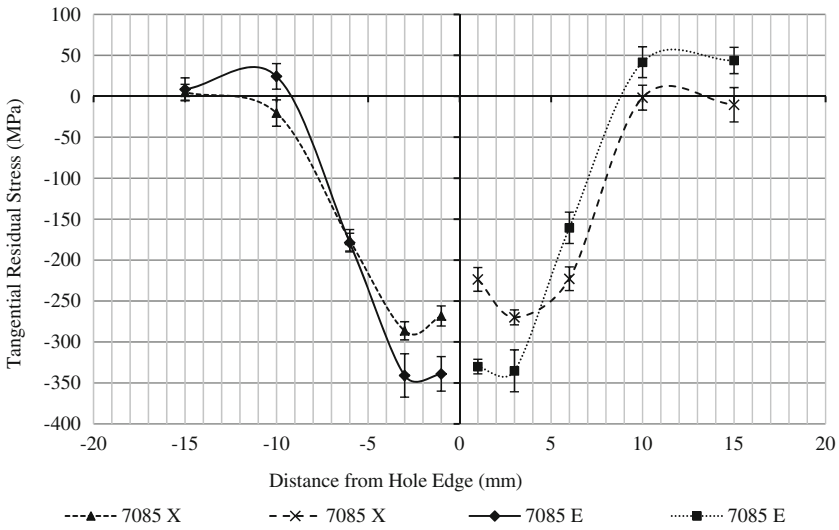

Fig. 12 Tangential residual stress along horizontal line through centre of hole for AA7085

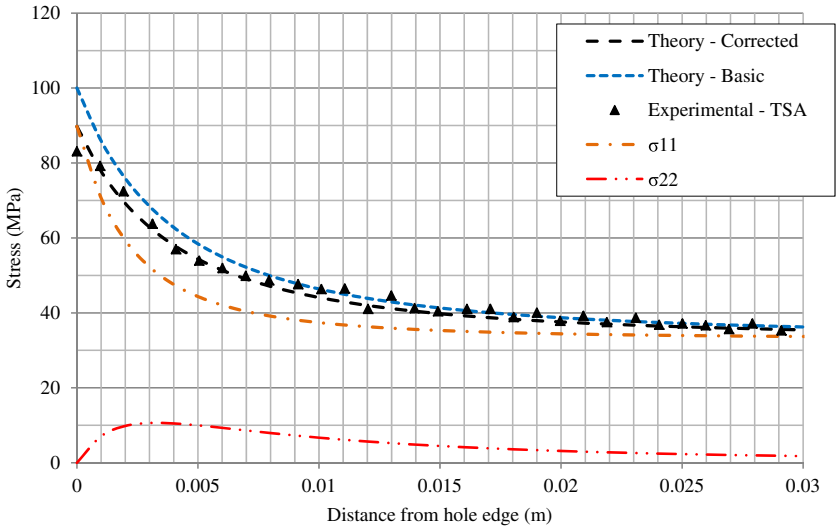

Fig. 13 Comparison of experimental (TSA) and theoretical stress distributions.

From Fig. 13 in can be deduced that although the plate is loaded uniaxially and there is no shear stress along the horizontal line through the hole, the system is not uniaxial since there is a significant contribution from σ_{22} near the hole. This may seem obvious, but the ramifications are such that equation (2) cannot be simplified and must be used in full when estimating the theoretical temperature change.

It has been shown that both the mean stress effect and the effect of plastic deformation on K, are evident in AA2024 and AA7085. Using the parameters obtained previously, combined with the stress distribution from the modified analytical solution, it is possible to assess the magnitude of the changes in ΔT that could be expected from either a change in mean stress, or such a change in α using equation (2). From such a study the dominant effect can be identified, and experimental TSA data from the 4 % cold expanded holes can be used for comparison. During the investigation of the temperature dependence of E the change in Poisson's ratio was also obtained, and no temperature dependence was found; therefore an assumption is made that Poisson's ratio does not change with temperature in the theoretical calculation of ΔT, i.e. $\partial\nu/\partial T = 0$.

For an AA2024 specimen aligned at 0° to the rolling direction containing 4 % plastic strain, a 2 % increase in K_P was measured. Assuming density and specific heat remain constant, this change in K_P represents a 2 % increase in α. Figure 14 shows the theoretical ΔT around the hole using equation (2), neglecting the effect of residual stress on the mean stress, for α_0, α_4, and α_{-4}, where the subscript denotes the amount of plastic strain for each value of α. The decrease in α used to model the effect of -4 % plastic strain has been defined as having the same magnitude as the increase for +4 % plastic strain. In Fig. 14, the modified α is only applied to the region effected by plastic deformation and is estimated as being between 0 mm and 8 mm from the hole; this approximation was based on the analysis of the thermoelastic and X-ray diffraction data. A small decrease in ΔT is predicted for the -4 % case, and a small increase is noted for the +4 % case. The experimental data around the 4 % cold expanded hole on the entry side of the AA2024 plate is also shown on Fig. 14, and it is clear that such a small change in α does not account for the decrease in ΔT measured close to the hole. Using equation (2) it is estimated that a 9 % change in α would be required to cause a decrease in ΔT that is equivalent to that obtained experimentally. Although this change is not dissimilar to that measured in the 45° AA2024 specimen, evidence suggests that the variation in thermoelastic response due to residual stress is not dominated by the change in α, and therefore the effect of including the residual stress in the mean stress term in equation (2) requires investigation.

The effective mean stress applied to the plates is a combination of the mean applied stress and the residual stress, i.e. $\sigma_{mean} = \sigma_{applied} + \sigma_{residual}$. Therefore the mean stress terms, σ_{kk}, σ_{11} and σ_{22}, have been modified to include both the applied mean stress based on the applied loading conditions, and the residual stresses obtained from X-ray diffraction. Since the contribution to residual stress due to cold rolling should be uniform for all plates, only the additional residual stress due to cold expansion has been considered in the analysis of changes in mean stress. Equation (2) is used to obtain theoretical values of ΔT for the case without expansion (0 %) and for the case with expansion (4 %). A third line of data is shown that accounts for the combined change in ΔT due to the additional residual stress measured from XRD and the change in α from plastic deformation. The results are plotted in Fig. 15(a), along with experimental TSA data from the 0 % and 4 % cold expanded holes for AA2024, entry side. The experimental TSA data around the 4 % and 0 % holes on the exit side of the AA2024 plate is shown in Fig. 15(b) and for both the entry and exit sides of the AA7085 plates in Fig. 15(c) and (d). These yield similar

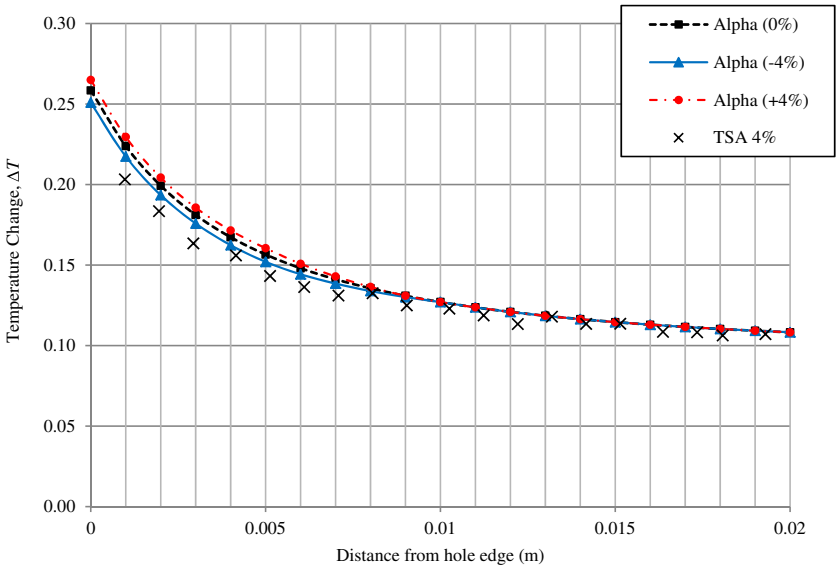

Fig. 14 Theoretical change in ΔT due to a change in α compared with experimental TSA data

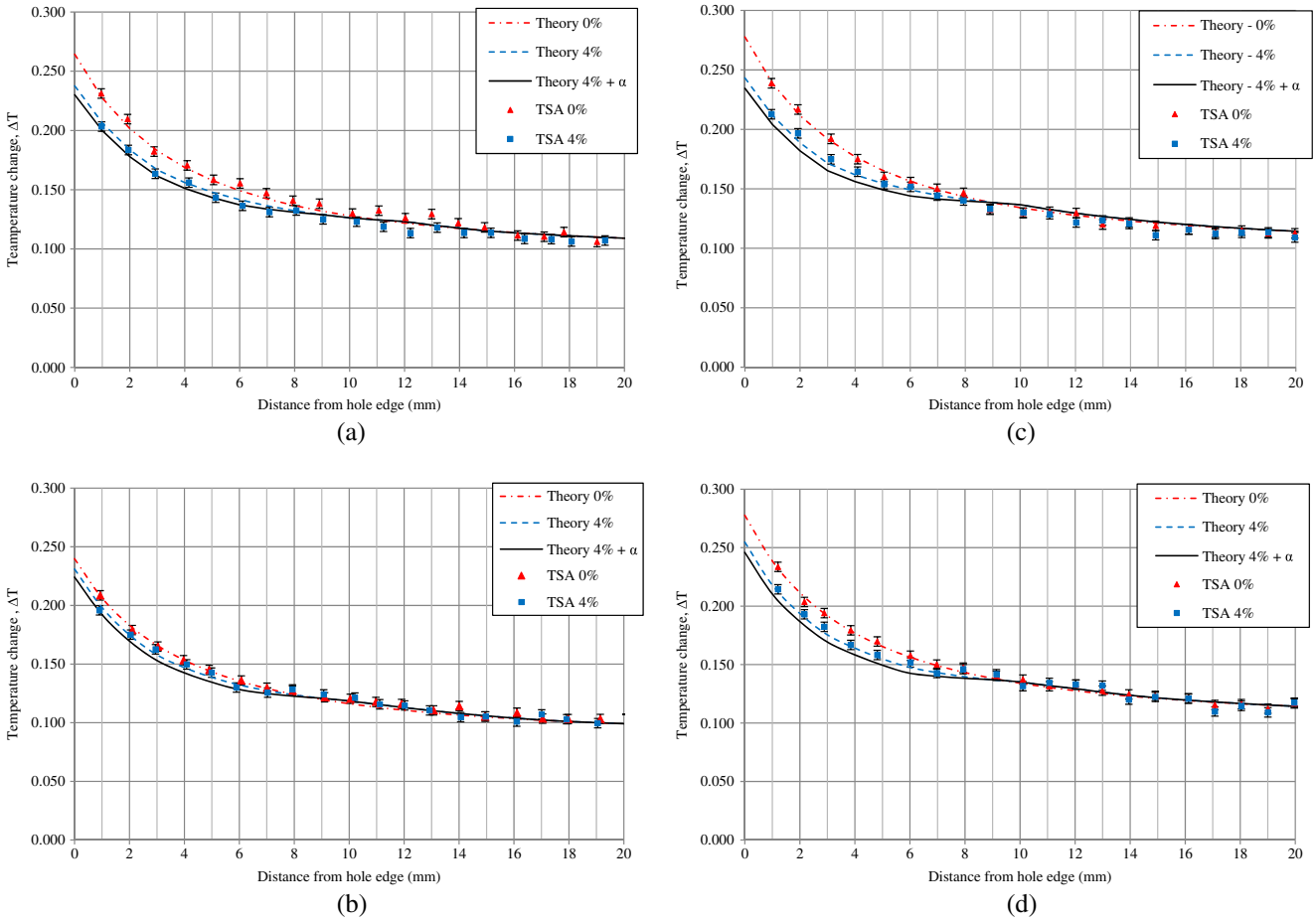

Fig. 15 **a** Theoretical change in ΔT due to incorporation of residual stress, and comparison with experimental ΔT data (AA2024 entry). **b** Theoretical change in ΔT due to incorporation of residual stress, and comparison with experimental ΔT data (AA2024 exit). **c** Theoretical change in ΔT due to incorporation of residual stress, and comparison with experimental ΔT data (AA7085 entry). **d** Theoretical change in ΔT due to incorporation of residual stress, and comparison with experimental ΔT data (AA7085 exit)

stress and temperature distributions to Fig. 15(a). However, there was discrepancy between the theoretical and experimental ΔT for the AA2024 exit side of the 0 % plate (Fig. 15b). This was corrected for by modifying the input stress data from the corrected analytical solution, so that ΔT in the region of uniform stress in the far field (0.05 m) was similar to the experimental response in the corresponding area. Hence it can be seen that the 0 % theory values are lower in Fig. 15(b) (AA2024 exit) than in Fig. 15(a) (AA2024 entry). Notwithstanding the small shift in the data in Fig. 15(b), the same trends are visible in all the plots in Fig. 15 with a clearly discernable difference between the data with and without the residual stress.

When the residual stress is included in the theoretical equations, then a reasonable fit is found with the experimental data for the 4 % cold expanded hole (i.e. the specimen with additional residual stress). When it is not included, a reasonable fit is seen with the experimental data for the 0 % cold expanded hole (i.e. the specimen without residual stress). It is interesting to note that the departures between the response for 0 % and 4 % become significantly smaller at approximately 8 mm, which correlates with the estimated areas of effect for both α and residual stress. When both the residual stress and a changing α are incorporated into equation (2), a good comparison between experimental and theoretical work can be made. However, due to the assumptions made with regards to the value of α, it is difficult to conclude which solution is most appropriate. Additionally, it can be seen that the effect of a large change in mean stress (i.e. the difference between the theoretical response for 0 % and 4 %) is greater than the effect of a change in α (difference between theoretical 4 % and 4 % + α). This would suggest that the change in ΔT due to residual stress is dominated by the mean stress effect as opposed to a change in α for AA2024. However, this assertion is based on results using an assumed change in α (for -4 % strain), and thus such a tendency is not necessarily the same for all materials.

It is encouraging that small variations in the thermoelastic response associated with residual stress have been identified from the neighbourhood of cold expanded holes. The residual stress field measured using X-ray diffraction has enabled theoretical predictions of ΔT that show good agreement with experimental results. However, the implication that the change in ΔT is dominated by the mean stress effect is significant. Since realistic components are likely to have multi-axial residual stress fields, as well as experiencing multi-axial loading scenarios, it is unlikely that any quantifiable components of residual stress could be calculated from a measured change in ΔT alone, due to the stress coupling in equation (2). However, it has been shown that when a known residual stress is included in a basic model, experimental TSA data correlates well with the theoretical temperature change. Thus, situations may arise where an elastic finite element model of the component may provide sufficient stress information to enable the components of residual stress to be estimated from equation (2). Nevertheless, it has been shown that if high residual stress exists, there is potential to measure a change in thermoelastic response, and subsequently identify the affected areas providing a reference specimen containing zero residual stress is available and the experimental conditions are carefully maintained.

Conclusions

Several previous studies have investigated residual stresses using TSA, but no successful approach for assessing residual stress has been established thus far. It was known that the presence of residual stress may influence the mean stress, providing an additional component of the thermoelastic signal. It was also shown that the application of plastic strain can modify the thermoelastic constant for some materials, resulting in a change in thermoelastic response. The well defined residual stress distribution around cold expanded holes presented an opportunity to investigate changes in thermoelastic response that occur as a result of residual stress, and assess the feasibility of using TSA as a potential residual stress assessment tool. Differences in the thermoelastic response were observed from around cold expanded holes in regions that would be expected to contain residual stress, and a rudimentary noise filter applied to identify areas where significant departures in thermoelastic response were measured.

Experimental work using tensile specimens revealed that plastic deformation did affect the thermoelastic constant for both materials, confirming that deformation experienced during cold expansion may cause changes in thermoelastic response around the holes. In addition, experimental work showed that the thermoelastic response of both materials was sensitive to the mean stress. The purpose of cold expansion is to create compressive residual stress around the hole, thus the 4 % hole contained residual stress from cold expansion *and* had experienced plastic deformation. In comparison, the 0 % hole did *not* contain residual stress from cold expansion and had *not* experienced any plastic deformation. Therefore there was the possibility that the change in response was due to the mean stress, the effect of plastic deformation, or a combination of the two.

Small but measurable differences in the thermoelastic response from areas that were known to contain different levels of residual stress were detected, and have been attributed to the increase in mean stress in those areas. The effect of α was noted, but the dominating contribution to the change in thermoelastic response appeared to be due to the mean stress effect in these materials. The ramifications suggest that it would be difficult to obtain any quantifiable residual stress information based on a measured change in thermoelastic response in a component with a non-uniform stress field. This questions the potential for TSA to be used for measuring residual stress, but does not completely rule

out its use in the field. The comparisons between TSA data from specimens with and without residual stress have only been possible due to the X-ray measurements of the residual stress. It is clear from this work that some additional or prior knowledge of either the residual stress distribution or a model of the loading conditions would always be required, regardless of the complexity of the case under investigation. This is a significant limitation, and prevents TSA being used as a stand-alone and quantitative measurement tool for residual stress evaluation. However, it is not unusual for comparisons to be made with stress free samples, or for analytical and finite element models to be used to provide insight into the analysis of measurements for other experimental techniques.

The work in the paper has shown that the thermoelastic response can be used to identify regions that have experienced residual stress. As discussed, quantifying these stresses may be difficult since a general component is complex with the mean applied stress, residual stress and cyclic stress all coupled. It is also the case that TSA is sensitive to experimental conditions, but if the approach could be improved it may provide a means of qualitatively identifying areas that contain residual stress that would be substantially quicker than currently available non-destructive techniques. However, some additional modelling or data from a stress free sample would be required to provide a comparison.

Finally, considering the magnitude of the temperature changes of interest, and the difficulty associated with measuring them, it is evident that TSA will not provide an immediate solution for a robust and portable means of residual stress measurement. However, the fact that measurable differences were obtained in areas where residual stress existed suggests there is still potential for TSA in the field of residual stress, albeit qualitatively. Furthermore, if the temperature resolution of infra-red detectors were to improve further, there may be opportunities for using TSA in conjunction with other techniques, and thus may provide an opportunity to enhance the current state of the art in residual stress assessment.

Acknowledgments The authors of this work would like to acknowledge Airbus for the provision of materials and assistance in cold hole expansion, and Judith Shackleton at the University of Manchester for support in obtaining X-ray diffraction residual stress measurements.

References

1. Dulieu-Barton J, Stanley P (1998) Development and applications of thermoelastic stress analysis. The Journal of Strain Analysis for Engineering Design 33(2):93–104
2. Wong AK, Sparrow JG, Dunn SA (1988) On the revised theory of the thermoelastic effect. J Phys Chem Solid 49(4):395–400
3. Pitarresi G, Patterson EA (2003) A review of the general theory of thermoelastic stress analysis. J Phys Chem Solid 38(5):405–417
4. Robinson AF, Dulieu-Barton JM, Quinn S, Burguete R (2009) A review of residual stress analysis using thermoelastic techniques. 7th International Conference on Modern Practices in Stress and Vibration Analysis, University of Cambridge, Sep 2009.
5. Wong AK, Dunn SA, Sparrow JG (1988) Residual stress measurement by means of the thermoelastic effect. Nature 332:613–615
6. Patterson E, Du Y, Backman D (2008) A new approach to measuring surface residual stress using thermoelasticity. Proceedings of SEM XI International Congress and Exposition, Orlando
7. Belgen MH (1967) Structural stress measurements with an infrared radiometer. ISA Trans 6:49–53
8. Machin AS, Sparrow JG, Stimson MG (1987) Mean stress dependence of the thermoelastic constant. Strain 23(1):27–30
9. Gyekenyesi AL (2002) Thermoelastic stress analysis: an nde tool for residual stress assessment in metallic alloys. Journal of Engineering for Gas Turbines and Power 124:383–387
10. Quinn S, Dulieu-Barton JM, Eaton-Evans J, Fruehmann RK, Tatum PJ (2008) Thermoelastic assessment of plastic deformation. The Journal of Strain Analysis for Engineering Design 43(6):451–468
11. Rosenholtz J, Smith D (1950) The effect of compressive stresses on the linear thermal expansion of magnesium and steel. J Appl Phys 21:396–399
12. Rosenfield AR, Averbach BL (1956) Effect of stress on the expansion coefficient. J Appl Phys 27:154–156
13. Quinn S, Dulieu-Barton JM, Langlands JM (2004) Progress in thermoelastic residual stress measurement. Strain 40(3):127–133
14. Landy MA, Champoux RL (1984) Fti engineering process specification fti 8101b—cold expansion of fastener and other holes using the split sleeve system (cx) and countersink cold expansion nosecap (ccx). Fatigue Technology Inc, Seattle
15. Ismonov S, Daniewicz SR, Newman JJC, Hill MR, Urban MR (2009) Three dimensional finite element analysis of a split-sleeve cold expansion process. J Eng Mater Tech 131(3):031007–031008
16. Ayatollahi MR, Arian Nik M (2009) Edge distance effects on residual stress distribution around a cold expanded hole in al 2024 alloy. Comput Mater Sci 45(4):1134–1141
17. Özdemir A, Edwards L (1996) Measurement of the three-dimensional residual stress distribution around split-sleeve cold-expanded holes. The Journal of Strain Analysis for Engineering Design 31(6):413–421
18. Gopalakrishna HD, Narasimha Murthy HN, Krishna M, Vinod MS, Suresh AV (2010) Cold expansion of holes and resulting fatigue life enhancement and residual stresses in al 2024 t3 alloy—an experimental study. Eng Fail Anal 17(2):361–368
19. Stanley P, Chan W (1986) 'Spate' stress studies of plates and rings under in-plane loading. Exp Mech 26(4):360–370
20. Belgen MH (1967) Infrared radiometric stress instrumentation application range study. NASA, 142, NASA Report CR-1067
21. Mckelvie J (1987) Consideration of the surface temperature response to cyclic thermoelastic heat generation. Proceed SPIE 731:44–53
22. Robinson AF, Dulieu-Barton JM, Quinn S, Burguete R (2010) Paint coating characterization for thermoelastic stress analysis of metallic materials. Meas Sci Tech 21(8):085502
23. Chicken J (2010) Private communication with manufacturer, FLIR
24. Gyekenyesi AL, Baaklini GY (1999) Thermoelastic stress analysis: the mean stress effect in metallic alloys. NASA, NASA-TM-1999-209376
25. Pilkey WD (1997) Peterson's stress concentration factors, 2nd edn. John Wiley & Sons
26. Folias ES, Wang JJ (1990) On the three-dimensional stress field around a circular hole in a plate of arbitrary thickness. Comput Mech 6(5):379–391
27. Ellyin F, Lind NC, Sherbourne AN (1966) Elastic stress field in a plate with a skew hole. J. Engng Mech. Div., Am. Soc. civ. Engrs 1:1–10
28. Sternberg E, Sadowsky MA (1949) Three-dimensional solution for the stress concentration around a circular hole in a plate of arbitrary thickness. J Appl Mech Trans ASME 16:27–38